S & M 4212

# Optimal Scheduling of Microgrid with Price–Incentive Coordinated Demand Response

Lingling Li,<sup>1,2</sup> Shirong Li,<sup>1,2</sup> Cheng-Jian Lin,<sup>3\*</sup> and Liyuan Zhao<sup>1,2</sup>

<sup>1</sup>State Key Laboratory of Intelligent Power Distribution Equipment and System, Hebei University of Technology, Tianjin 300401, China

<sup>2</sup>Key Laboratory of Electromagnetic Field and Electrical Apparatus Reliability of Hebei Province, Hebei University of Technology, Tianjin 300401, China
<sup>3</sup>Department of Electronic Engineering, National Chin-Yi University of Technology, Taichung 41170, Taiwan

(Received July 23, 2025; accepted September 30, 2025)

Keywords: microgrid, demand response, PIC-DR, sensor, scheduling

A coordinated optimization framework that integrated the price-incentive collaborative demand response (PIC-DR) mechanism and the improved dream optimization algorithm (IDOA) was proposed to address scheduling challenges caused by renewable energy volatility and the demand response in microgrids. First, a dual-track demand response mechanism was designed, that is, time-of-use pricing-guided load shifting, while dynamic incentive compensation enhanced user participation, thereby establishing a scheduling architecture that balanced economic efficiency with response reliability. Next, IDOA was introduced, incorporating a logistic map chaos perturbation mechanism to strengthen its global search capability and an adaptive dream-intensity strategy to balance exploration and exploitation, which significantly improved solution efficiency for high-dimensional constrained problems. Finally, the framework was validated using sensor-measured data from a residential microgrid in North China under gradient-based participation scenarios (0, 50, and 100%). The results demonstrated that, on the Congress on Evolutionary Computation (CEC) test functions F8-F13, IDOA improved convergence accuracy by one to three orders of magnitude compared with traditional algorithms. Under full demand response participation, operational costs decreased by 27.5% and the peak-tovalley load difference decreased by 41.2%. The PIC-DR mechanism achieved a peak load shift of 18.7% through dynamic incentives, effectively mitigating renewable energy volatility. The study thus provided an economically efficient scheduling paradigm for microgrids with high renewable energy penetration.

### 1. Introduction

With the increasing global focus on environmental protection and the intensification of the energy crisis, traditional energy supply methods are facing significant challenges. (1,2) The over-reliance on fossil fuels raises concerns about resource depletion and leads to severe air pollution and greenhouse gas emissions. In response to this predicament, there is a global push for the

\*Corresponding author: e-mail: <a href="mailto:cjlin@ncut.edu.tw">cjlin@ncut.edu.tw</a>
<a href="mailto:https://doi.org/10.18494/SAM5857">https://doi.org/10.18494/SAM5857</a>

transformation of the energy structure, with renewable energy emerging as a key alternative. (3) In particular, continuous advancements in technologies for renewable energy sources such as wind and solar power make them mainstream in electricity generation. (4) However, despite the widespread adoption of renewable energy globally, its volatility and uncertainty present new challenges for traditional power systems. (5) Conventional centralized grids often fail to effectively cope with the intermittent supply of renewable energy, leading to stability and reliability issues within the power system.

Microgrids (MGs), as an emerging energy management system, have become an effective solution to addressing these challenges. They offer flexible energy scheduling capabilities through the incorporation of diverse distributed energy technologies, such as wind power, solar power, and energy storage systems, which allow them to maintain a stable power supply while enhancing energy efficiency. In addition, advanced sensor networks—comprising voltage, current, temperature, and power-quality sensors—provide real-time monitoring and data acquisition, providing IoT-based control algorithms that enable the rapid detection of system fluctuations and rapid responses to them. MGs not only optimize the configuration of local energy resources but also implement load management and the demand response (DR) through intelligent scheduling systems that rely on continuous sensor feedback. Through the proper regulation of DR guided by accurate sensor measurements, MGs can automatically adjust energy output during supply—demand imbalances, preventing energy waste or shortages, while reducing reliance on traditional energy sources and promoting the development of a low-carbon economy. (10)

Currently, the optimal scheduling of MGs has been widely researched. Ramkumar *et al.*<sup>(11)</sup> proposed the energy management scheme for multi-energy microgrids (MEMGs) based on quadratic interpolation, the grey goose optimization new local search (QI-NLS-G2O), and the Gaussian radius zone perception network (GRZPNet), aiming to optimize scheduling strategies, mitigate renewable energy uncertainty, and improve system performance. Nandish and Pushparajesh<sup>(12)</sup> proposed a load scheduling method based on the adaptive whale optimization algorithm (AWOA), using an agent-based system to identify priority versus nonpriority loads and interacting with smart MGs to reduce losses, enhance grid efficiency, and lower users' electricity costs. Qi and Su<sup>(13)</sup> proposed an integrated power—thermal—gas energy-system optimization model that considers uncertain indirect carbon emission intensity, addressing challenges posed by renewable energy volatility in low-carbon economic scheduling. Ju *et al.*<sup>(14)</sup> introduced an improved honey-badger algorithm (MHBA) within a probabilistic MG energy-management framework to optimize overall MG operation.

DR can be classified into two categories based on the response approach: price-based demand response (PBDR) and incentive-based demand response (IBDR). Thang *et al.* Proposed a day-ahead integrated DR strategy for energy MGs that considered adjustable loads, aiming to optimize the energy consumption structure through time-of-use (TOU) pricing. Wang and Li addressed the limitations of existing MG-DR models, further optimized flexible load control strategies, and proposed a dual-objective optimization model based on electricity-price signals and incentives. Liu *et al.* Increased the scheduling flexibility of photovoltaic (PV) storage systems by integrating DR, encouraging source-load participation in peak shaving and valley

filling, thereby improving the renewable energy absorption capacity of PV storage MGs and enhancing their economic and social benefits. Wang *et al.*<sup>(20)</sup> explored the potential interaction between electric–thermal flexible loads and energy MGs by combining the integrated demand response (IDR), and proposed an optimal scheduling model based on chance-constrained programming (CCP).

In summary, MGs demonstrate significant advantages in enhancing energy-utilization efficiency and economic benefits. However, the collaborative optimization mechanism of economic and environmental benefits within the multi-energy coordination framework remains underdeveloped. Specifically, existing research predominantly focuses on single-energy scheduling or independent DR strategies, leaving a notable gap in the field of collaborative optimization between MG scheduling and DR. With the growing scale of MGs, effectively managing fluctuations in renewable energy generation and load demand through DR technology has become a critical challenge that needs urgent attention in MG optimization scheduling.

In this paper, we propose a price—incentive coordinated demand response (PIC-DR) mechanism to optimize MG scheduling. The PIC-DR mechanism synergistically combines TOU pricing with targeted incentive compensation to effectively guide user behavior: TOU pricing encourages load shifting to off-peak periods, whereas direct incentives motivate specific, critical demand reductions or participation in ancillary services when needed. The improved dream optimization algorithm (IDOA) was also utilized to achieve an economically optimal schedule. The main contributions of this study are as follows.

- (1) A novel PIC-DR mechanism was proposed to overcome the limitations of PBDR and IBDR. By organically combining TOU pricing with dynamic incentive compensation, we established this DR framework that better aligns with actual user behavior and exhibits stronger responsiveness. The framework effectively improved its capability to mitigate the volatility of renewable energy output and sudden load-demand fluctuations, while reducing its economic costs.
- (2) A novel IDOA was proposed, which introduced a chaotic perturbation mechanism and adaptive dream intensity control. During the dream phase, a logistic map chaos perturbation was employed to generate disturbance coefficients, preventing premature convergence and enhancing global search capability. A nonlinear decay strategy for dream intensity was also introduced to dynamically balance exploration and exploitation, thereby significantly improving convergence speed and solution accuracy.
- (3) A collaborative optimization framework was constructed and validated. An economic scheduling optimization model for the MG was developed on the basis of the PIC-DR mechanism and IDOA. Comparative scenarios with varying levels of DR participation were designed. The results quantitatively demonstrated that increased user participation significantly reduced the MG's overall economic cost and improved operational stability, empirically validating the superiority of the proposed method.

The structure of the remaining parts of this study is as follows. In Sect. 2, we describe the system architecture and establish the MG economic scheduling optimization model. In Sect. 3, IDOA is proposed. In Sect. 4, we conduct a case study to validate the effectiveness of the PIC-DR mechanism and IDOA. Finally, in Sect. 5, we provide conclusions and a future outlook.

## 2. System Model

## 2.1 System structure

In this section, we provide a detailed description of the MG economic scheduling optimization model. The MG under study operates in a grid-connected mode. To ensure real-time power balance, the MG can engage in bidirectional electricity trading with the distribution network. Figure 1 illustrates the structural diagram of the MG system. The system integrates wind power generation, PV generation, fuel cells, and battery energy storage. A central control center orchestrates the operation of these components and manages the power exchange interface with the distribution network. The wind turbine (WT) system, equipped with wind speed and direction sensors, gearbox vibration monitors, and generator speed sensors, provides critical data for wind power forecasting and operational monitoring. The PV system utilizes irradiance and back-side temperature sensors to support accurate solar power generation prediction. The fuel cell system incorporates hydrogen pressure, fuel cell stack temperature, and output voltage/current sensors; this comprehensive instrumentation enables the real-time analysis of reaction efficiency, health status assessment, and precise power output control. The battery storage system similarly employs sensors for monitoring and management.

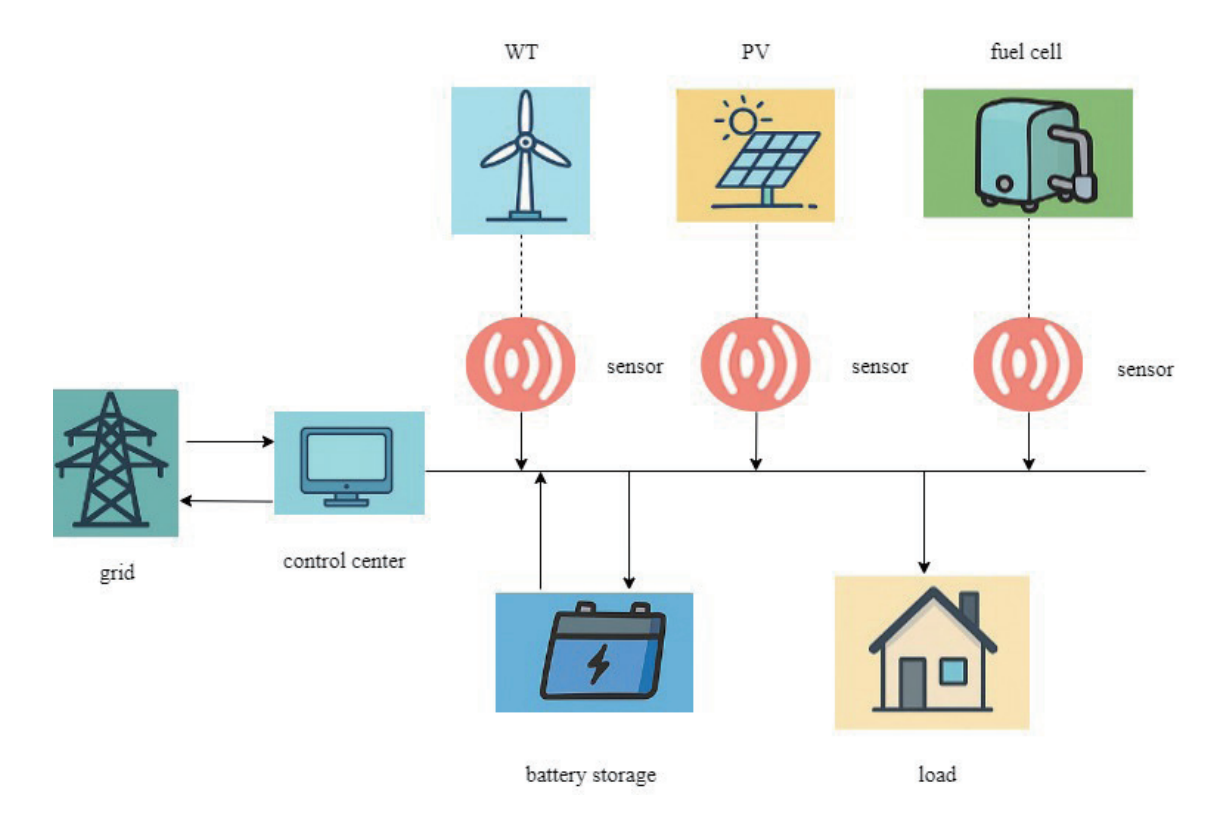


Fig. 1. (Color online) MG structure diagram.

## 2.2 Optimization model

#### 2.2.1 Objective function

In this study, we constructed the objective function by considering the comprehensive economic costs of the MG. The economic costs include those of purchasing electricity, investments, operation and maintenance, fuel, and compensation for demand-side load shifting.

$$F = \sum_{t=1}^{T} \left[ C_{Grid} + C_{In} + C_{Om} + C_{Fc} + C_{DR} \right], \tag{1}$$

where  $C_{Grid}$ ,  $C_{In}$ ,  $C_{Om}$ ,  $C_{Fc}$ , and  $C_{DR}$  are the electricity purchase, investment, operation and maintenance, fuel, and demand-side load shifting compensation costs, respectively.

$$C_{Grid} = P_{buv}(t)C_{buv}(t) - P_{sell}(t)C_{sell}(t), \qquad (2)$$

where  $C_{buy}(t)$  and  $C_{sell}(t)$  are the electricity purchase and sale costs from the MG to the distribution network, and  $P_{buy}(t)$  and  $P_{sell}(t)$  are the electricity purchase and sale power from the MG to the distribution network, respectively.

$$C_{In} = \sum_{\tau \in \Phi} \frac{r(1+r)^{n_{\tau}}}{(1+r)^{n_{\tau}} - 1} \cdot I_{\tau} \cdot C_{\tau}^{cap} , \qquad (3)$$

where  $C_{\tau}^{cap}$  is the installed capacity of the equipment,  $I_{\tau}$  is the installation cost per unit of capacity,  $n_{\tau}$  is the average lifespan of the equipment, and r is the discount rate.

$$C_{Om} = \sum_{\tau \in \Phi} K_{Om}^{\tau} \cdot P_{\tau}(t) , \qquad (4)$$

where  $K_{Om}^{\tau}$  is the operation and maintenance coefficient of the equipment and  $P_{\tau}(t)$  is the output power of the MG's equipment at time t.

$$C_{DR} = \sum_{k=1}^{M} \sum_{t=1}^{T} \sum_{i=1}^{T} \varepsilon_{DR} \cdot Q_{DR}^{k}(t, t'),$$
 (5)

where  $\varepsilon_{DR}$  is the cost of compensation of the demand-side users per unit of time and  $Q_{DR}^k$  is the amount of demand response load shifting.

## 2.2.2 Constraint

To ensure a reliable and safe power supply, the generating units of the MG must maintain the following balance.

Power balance constraint

$$P_{PV}(t) + P_{WT}(t) + P_{FC}(t) + P_{grid,buv}(t) - P_{grid,sell}(t) = P_{load}(t)$$

$$\tag{6}$$

Energy storage system constraint

$$SOC_{min} \leq SOC(t) \leq SOC_{max}$$
 (7)

Energy interaction constraint between MGs and distribution grids

$$P_{grid,min} \leqslant P_{grid} \leqslant P_{grid,max} \tag{8}$$

Power constraints for each distributed power source

$$P_{i,min} \leqslant P_i \leqslant P_{i,max} \tag{9}$$

## 3. Optimization Method

The dream optimization algorithm (DOA) is a swarm intelligence method simulating the sleep-dream process, known for its strong spatial exploration capabilities. However, DOA suffers from slow convergence and reduced solution accuracy in high-dimensional, constrained search spaces. Crucially, the PIC-DR scheduling model presents precisely such a challenge: it is a high-dimensional problem with complex operational constraints. To overcome DOA's limitations for this specific application, we propose an IDOA, specifically enhancing global search and convergence efficiency. Figure 2 illustrates the IDOA flow. In the following section, we detail the algorithmic improvements and implementation framework.

#### 3.1 Chaotic perturbation mechanism

To address the issue of DOA getting trapped in local optima during the dream phase, we introduce a logistic chaos mapping to generate perturbation coefficients in the dream phase, thereby enhancing population diversity and improving global search capability. The chaotic perturbation mechanism is implemented as follows.

Logistic chaos sequence generation:

$$\varphi_{k+1} = \mu \cdot \varphi_k \cdot (1 - \varphi_k), \quad \varphi_k \in (0,1), \tag{10}$$

where  $\mu$  is the chaotic parameter and  $\varphi_k$  is the random initial value.

The dream perturbation formula is as follows.

In the dream phase of DOA, chaotic perturbation is applied to the current individual position  $x_i^t$ :

$$x_i^{new} = x_i^t + \beta \cdot (2\varphi_k - 1) \cdot (x_{max} - x_{min}), \tag{11}$$

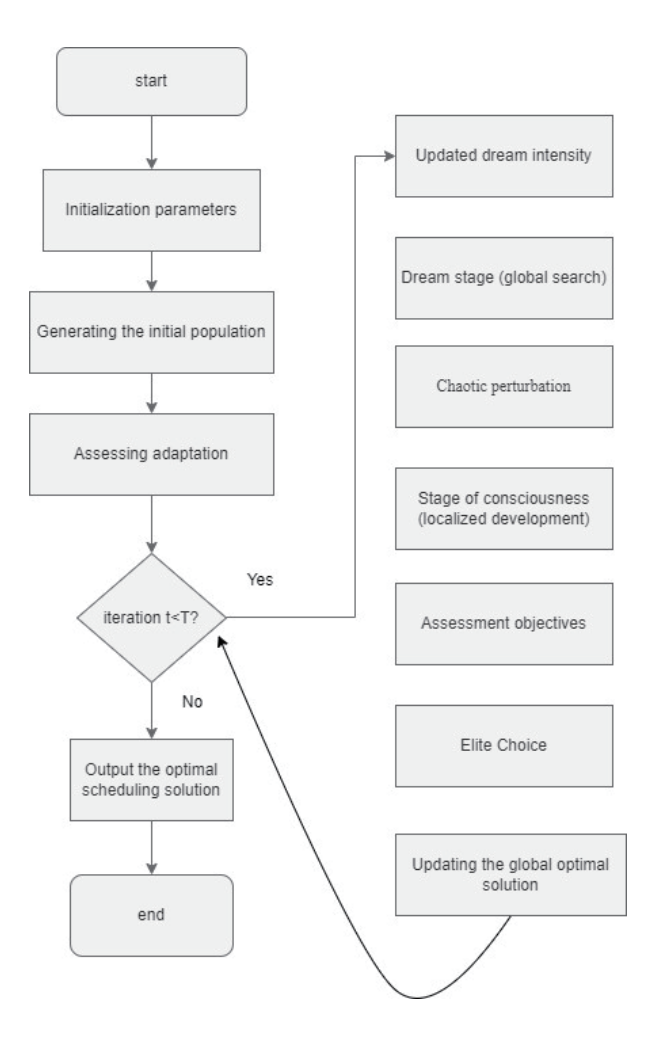


Fig. 2. (Color online) Flowchart of IDOA.

where  $\beta$  is the perturbation intensity coefficient,  $x_{max}$  and  $x_{min}$  are the upper and lower bounds of the decision variables, respectively, and  $(2\varphi_k - 1)$  maps the chaotic variable to the interval [-1, 1], enabling bidirectional perturbation.

## 3.2 Adaptive dream intensity control

To address the issue of the fixed parameters in DOA failing to balance "exploration-exploitation", a nonlinear decay strategy for dream intensity is proposed:

$$\alpha(t) = \alpha_{min} + (\alpha_{max} - \alpha_{min}) \cdot e^{-\lambda \cdot (t/T_{max})}, \qquad (12)$$

where  $\alpha_{max}$  and  $\alpha_{min}$  are the intensity boundaries,  $\lambda$  is the decay rate factor, t is the current iteration count, and  $T_{max}$  is the maximum number of iterations.

In the core update formula of DOA, the exploration step size is dynamically controlled as

$$x_i^{t+1} = x_i^t + \alpha(t) \cdot \left[ R_1 \cdot (x_{best} - x_i^t) + R_2 \cdot (x_{r1} - x_{r2}) \right], \tag{13}$$

where  $R_1$  and  $R_2 \sim U(0,1)$  are random numbers, and  $x_{best}$  is the current optimal solution.

## 4. Case Analysis

### 4.1 Basic data

To verify the effectiveness of IDOA, in this study, we select a residential community in a region of North China as the research subject. The MG system's electricity purchase and sale prices at different times within 24 h, along with the parameters of each device, are shown in Tables 1 and 2.

Table 1 shows the electricity purchase and sale prices for each time over 24 h, whereas Table 2 presents the operational parameters of various devices in the MG system, including power limits, operation and maintenance costs, investment costs, efficiency, ramp-up rate, and lifetime. In this study, we used the aforementioned data as inputs and performed a 24 h economic scheduling simulation for the residential MG system with a 1 h scheduling interval. During the system's operation cycle, all generating units and storage devices operate according to the parameters in the tables. To maximize the utilization of renewable energy, priority is given to PV and WT generation. Figure 3 shows the typical daily output power of PV and WT, whereas Fig. 4 illustrates the TOU electricity price curves for electricity purchase and sale.

Table 1
Prices of purchasing and selling electricity.

Items	Time interval	Price
	0:00-7:00	0.45
Price of purchasing	8:00-10:00, 14:00-16:00, 21:00-23:00	0.8
	11:00-13:00, 17:00-20:00	1.36
	0:00-7:00	0.35
Price of selling	8:00-10:00, 14:00-16:00, 21:00-23:00	0.58
	11:00-13:00, 17:00-20:00	1.15

Table 2 Unit equipment operating parameters.

Figure	ESS	FC	PV	WT
Lower power limit (kW)	-100	0	0	0
Upper power limit (kW)	120	160	150	100
Operation and maintenance cost (yuan·kW)	0.02	0.0287	0.085	0.25
Total investment cost (yuan)	700	1500	3000	6000
Efficiency	0.85	0.6	_	_
Ramp-up rate (kW)	20	20	_	_
Lifetime (year)	20	15	20	20

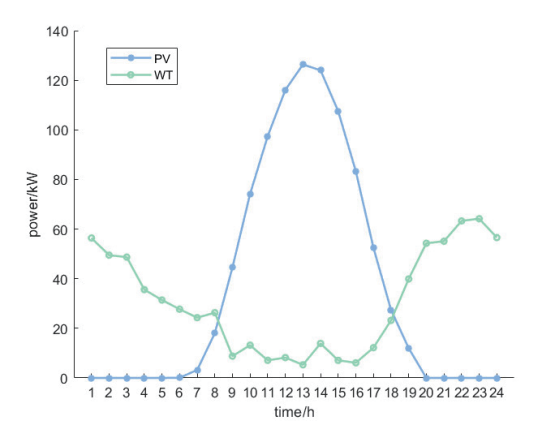


Fig. 3. (Color online) Typical daily power outputs of PV and WTs.

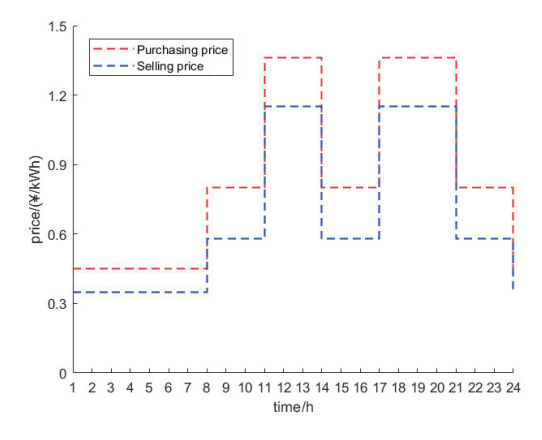


Fig. 4. (Color online) TOU electricity prices for electricity purchase and sale.

#### 4.2 Performance test and analysis

To verify the performance of IDOA, we selected the F8–F13 functions from the Congress on Evolutionary Computation (CEC) test suite and compared them with those of DOA, the grasshopper optimization algorithm (GOA), and the whale optimization algorithm (WOA). To ensure a fair comparison with other algorithms while balancing convergence speed and global search capability, the following settings were applied to the key parameters of IDOA: the population size for each algorithm was set to 50, the number of iterations was 300, and each test function was independently run 30 times for each algorithm.

As shown in Fig. 5, IDOA demonstrates robust convergence across the six benchmark functions F8–F13. It not only converges quickly but also achieves high convergence accuracy. Table 3 shows that, in 30 independent experiments, the global optimal solution search accuracy of IDOA significantly outperforms those of the compared algorithms.

### 4.3 Case results and analysis

On the basis of IDOA, we designed three sets of gradient-based demand response participation scenarios. By the comparative analysis of the dynamic evolution of MG scheduling

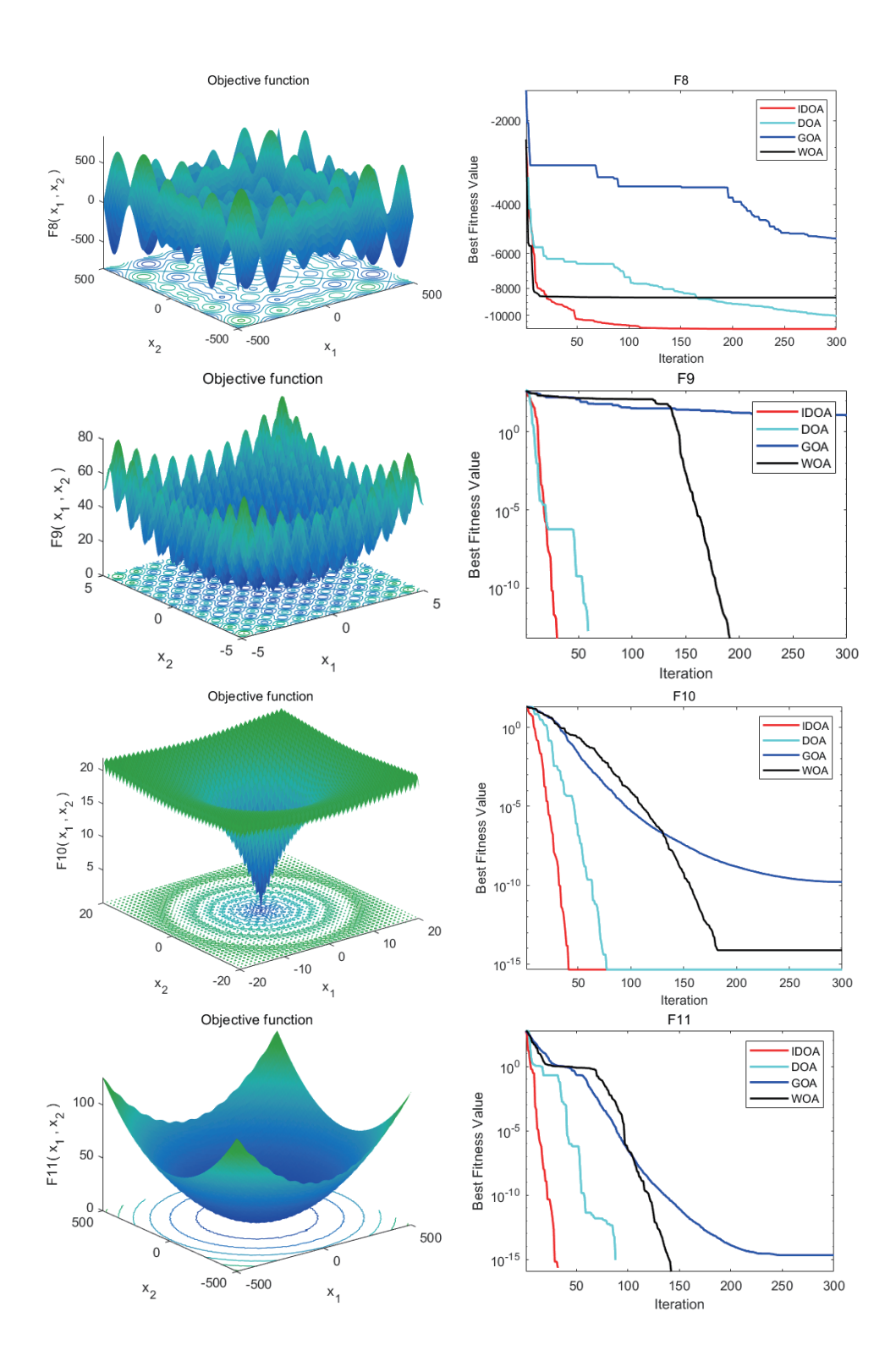


Fig. 5. (Color online) Tests with different algorithms under F8–F13.

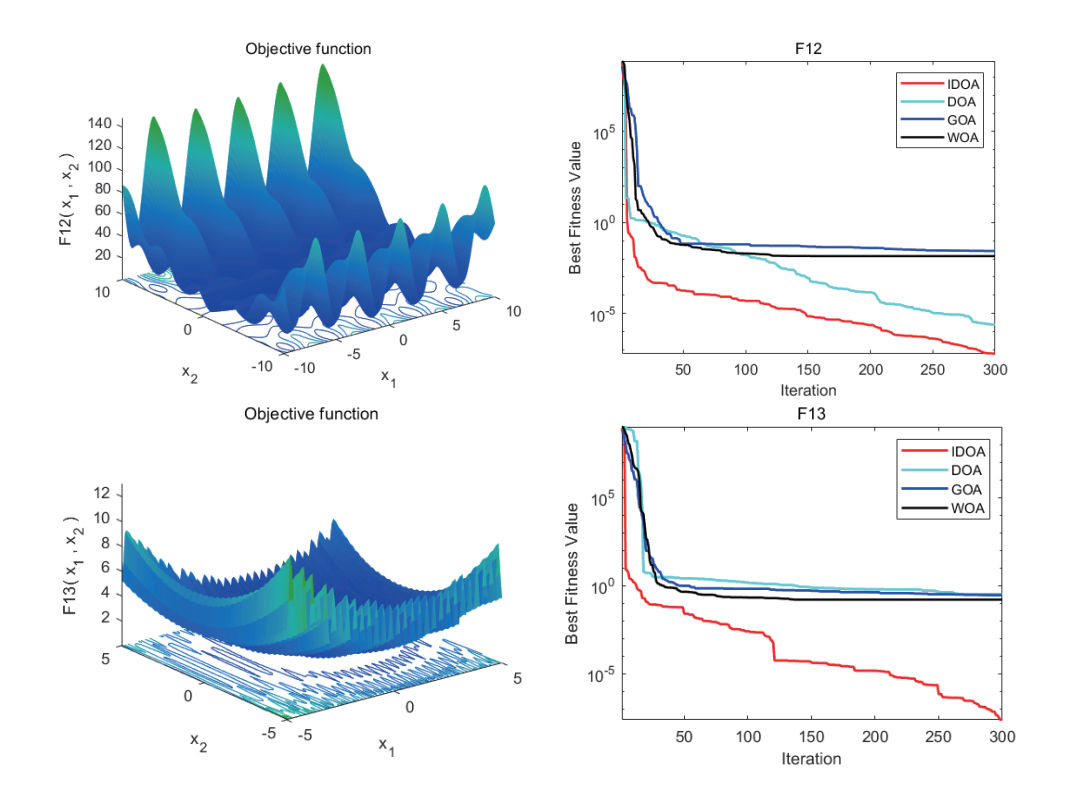


Fig. 5. (Color online) (Continued) Tests with different algorithms under F8–F13.

Table 3 Results of tests using different algorithms.

Function		IDOA	DOA	GWO	WOA
F8	best	-1.12E+04	-1.00E+04	-5.30E+03	-8.63E+03
	mean	3.62E+02	1.19E+03	1.05E+03	1.78E+03
F9	best	0	0	1.22E+01	0
	mean	0	2.79E+01	2.12E+01	0
F10	best	4.44E-16	4.44E-16	1.60E-10	7.55E-15
	mean	4.44E-16	4.44E-16	1.06E-10	1.87E-15
F11	best	0	0	2.11E-15	0
	mean	0	1.94E-02	8.13E-03	0
F12	best	5.99E-08	2.40E-06	2.71E-02	1.42E-02
	mean	3.35E-08	2.05E-06	1.78E-02	1.09E-02
F13	best	2.40E-08	3.21E-01	2.84E-01	1.59E-01
	mean	9.62E-07	1.21E-01	1.80E-01	1.27E-01

schemes, we quantitatively revealed the impacts of user demand response participation rate on system economics and operational stability. The scenario construction follows the principle of controlling variables: under the fixed boundary conditions, such as renewable energy output and TOU pricing mechanisms, the impact of user participation in demand response on MG scheduling is analyzed.

- Case 1: No users participate in demand response.
- Case 2: 50% of users participate in demand response.
- Case 3: All users participate in demand response.

As shown in Fig. 6, when no users participate in demand response, the typical daily load curve exhibits a "double-peak" characteristic. Between 1:00 AM and 7:00 AM, there is a dual low period for both power demand and market electricity prices, making this the optimal window for battery energy storage system (BESS) charging. After the load begins to rise, BESS switches to the discharge state to provide additional power to the MG. The scheduling scheme primarily meets the MG's demand in the following ways: during the peak electricity demand, the MG purchases electricity from the distribution network, and during the low electricity demand, it sells power to the distribution network, prioritizing the consumption of renewable energy. Additionally, during high-electricity-price periods, BESS is used to provide power. Throughout the scheduling process, renewable energy and fuel cells (FCs), along with BESS for storage and discharge, are utilized, allowing the MG to achieve optimal scheduling through reasonable electricity purchase and sale.

Figure 7 shows the optimization scheduling results of the MG when 50% of users participate in demand response. It can be observed that, owing to user participation in demand response, the peak-to-valley difference of the load curve decreases. The amount of power sold by the MG to the distribution network has increased compared with the previous scenario, and the electricity stored by BESS during the early hours has decreased.

As shown in Fig. 8, after all users participate in demand response, further optimization of the system's scheduling is achieved. The peak-to-valley difference of the load curve significantly decreases, showing a smoother trend, and reduces the peak-to-valley load difference by 41.2%, with a peak load shift of 18.7%. The electricity stored by BESS during low-electricity-price periods decreases, and more power is provided by BESS during high-electricity-price periods. Additionally, the MG sells more power to the distribution network, realizing optimal economic cost scheduling.

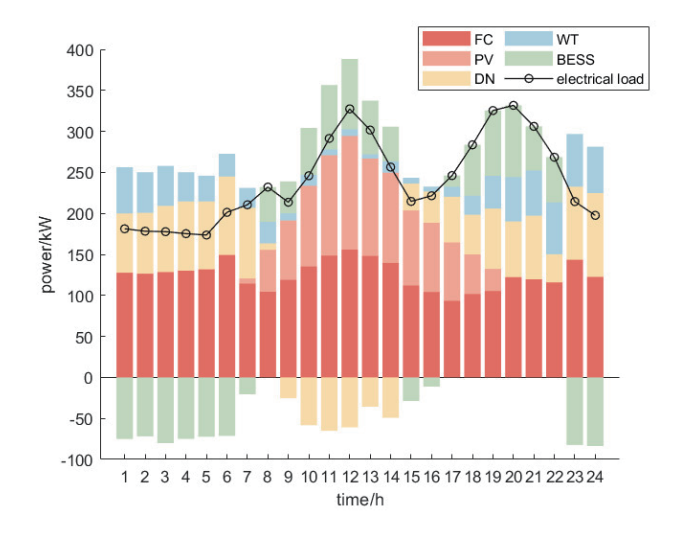


Fig. 6. (Color online) Scheduling results for Case 1.

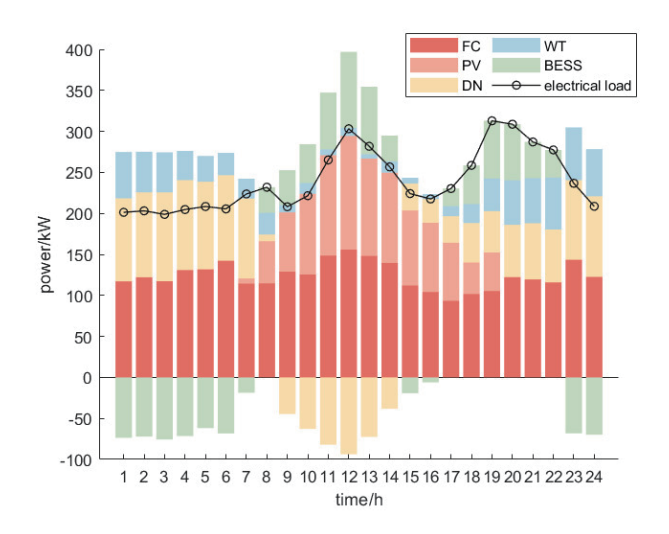


Fig. 7. (Color online) Scheduling results for Case 2.

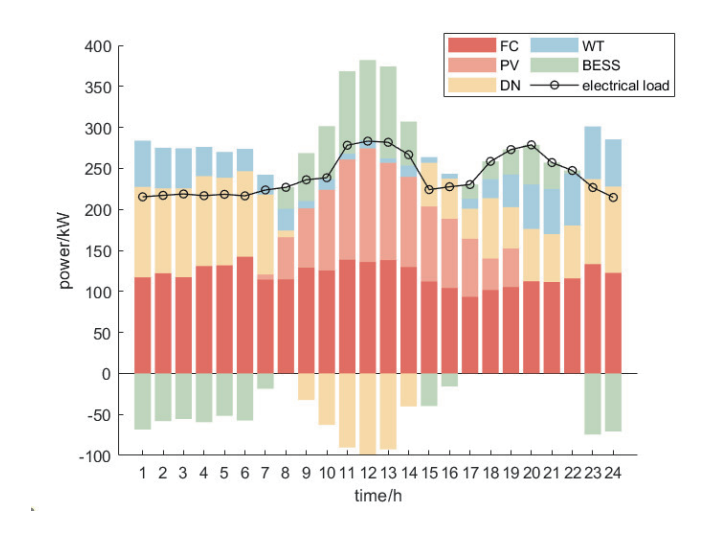


Fig. 8. (Color online) Scheduling results for Case 3.

Table 4
Economic costs for different scenarios.

Scenario	Cost
Case 1	17651.33
Case 2	14872.35
Case 3	12784.76

Table 4 shows the economic costs of the MG under three different scenarios. It can be observed that after users actively participate in demand response, the MG experiences a reduction in load during peak-electricity-demand periods, while the power sold to the distribution network increases. This demonstrates that the optimization strategy can significantly reduce the economic costs of the MG.

### 5. Conclusions

In this study, we focused on the economic scheduling of MGs, achieving the coordinated optimization of both economic efficiency and stability through innovative mechanisms and algorithm improvements. The main conclusions are as follows.

- (1) Effectiveness of the PIC-DR Mechanism: The PIC-DR framework, combining TOU pricing and dynamic incentives, reduces system costs by 27.5% and peak-to-valley load difference by 41.2%, with a peak load shift of 18.7%, mitigating renewable energy fluctuations.
- (2) Performance of IDOA: IDOA, with chaotic disturbance and adaptive dream intensity control, improves convergence accuracy by 1–3 orders of magnitude and speeds up iteration by 40% on CEC high-dimensional test functions, solving complex MG scheduling in 2.8 s on average.
- (3) Impact of User Participation: Comparative experiments show a strong correlation between user participation rate and system economics/stability, offering a theoretical basis for precise MG demand response control.

Future research can integrate blockchain technology to enable decentralized demand response trading, further reducing incentive costs.

## Acknowledgments

This study was supported by the Tianjin Carbon Peak and Carbon Neutrality Technology Major Project (Grant No. 24ZXTKSN00030) and Tianjin Natural Science Foundation Project (Grant No. 23JCQNJC01060)

#### References

- W. Y. Liu, C. Q. Rui, Z. L. Liu, and J. X. Chen: Case Stud. Therm. Eng. 69 (2025) 105937. <a href="https://doi.org/10.1016/j.csite.2025.105937">https://doi.org/10.1016/j.csite.2025.105937</a>
- D. H. Wei, L. Y. Zhang, N. Zhang, J. L. Fang, and Q. Qian: J. Cleaner Prod. 421 (2023) 138531. <a href="https://doi.org/10.1016/j.jclepro.2023.138531">https://doi.org/10.1016/j.jclepro.2023.138531</a>
- 3 Y. B. Zheng, X. Xue, S. Xi, and W. Xin: J. Cleaner Prod. **450** (2024) 141691. <a href="https://doi.org/10.1016/j.jclepro.2024.141691">https://doi.org/10.1016/j.jclepro.2024.141691</a>
- 4 S. Govindasamy, S. R. Balapattabi, B. Kaliappan, and V. Badrinarayanan: Electr. Eng. 105 (2023) 4409. <a href="https://doi.org/10.1007/s00202-023-01947-8">https://doi.org/10.1007/s00202-023-01947-8</a>
- 5 D. Z. Wang, X. L. Gao, L. Han, Z. H. Xiao, T. Feng, and J. F. Wu: 2024 7th Asia Conf. Energy and Electrical Engineering, ACEEE 2024 (2024) 195. https://doi.org/10.1109/Aceee62329.2024.10651763
- 6 X. H. Zhang, J. L. Ramírez-Mendiola, Y. Q. Lai, J. Z. Su, M. T. Li, and L. J. Guo: Energy Convers. Manage. 287 (2023) 117099. <a href="https://doi.org/10.1016/j.enconman.2023.117099">https://doi.org/10.1016/j.enconman.2023.117099</a>
- 7 P. A. Prassath and M. Karpagam: Environ. Dev. Sustainability 26 (2024) 31465. <a href="https://doi.org/10.1007/s10668-024-04499-4">https://doi.org/10.1007/s10668-024-04499-4</a>
- 8 Y. Zhao, W. Wang, Y. B. Wang, and X. H. Chen: 2022 12th Int. Conf. Power and Energy Systems, Icpes (2022) 417. https://doi.org/10.1109/Icpes56491.2022.10072591
- 9 J. Zhu, Y. H. Jin, W. H. Zhu, D. K. Lee, and N. Bohlooli: Int. J. Hydrogen Energy **114** (2025) 354. <a href="https://doi.org/10.1016/j.ijhydene.2025.02.354">https://doi.org/10.1016/j.ijhydene.2025.02.354</a>
- 10 L. Y. Liu, X. W. Shen, Z. G. Chen, Q. Sun, and R. Wennersten: IEEE Access 12 (2024) 102061. <a href="https://doi.org/10.1109/Access.2024.3432120">https://doi.org/10.1109/Access.2024.3432120</a>
- 11 M. S. Ramkumar, J. Subramani, M. Sivaramkrishnan, A. Munimathan, G. K. O. Michael, and M. M. Alam: Sci. Rep. 15 (2025) 7755. https://doi.org/10.1038/s41598-025-90062-8
- 12 B. M. Nandish and V. Pushparajesh: Electr. Eng. 106 (2024) 4439. https://doi.org/10.1007/s00202-023-02214-6
- 13 N. Qi and J. Su: Iet Gener. Transm. Distrib. 19 (2025) e70014. https://doi.org/10.1049/gtd2.70014

- 14 Y. F. Ju, S. F. Wang, J. Ren, L. G. Wang, and A. N. Abdalla: Int. J. Hydrogen Energy **136** (2025) 609. <a href="https://doi.org/10.1016/j.ijhydene.2025.04.471">https://doi.org/10.1016/j.ijhydene.2025.04.471</a>
- T. Bal, S. Ray, N. Sinha, R. Devarapalli, and L. Knypinski: Energies 16 (2023) 5767. <a href="https://doi.org/10.3390/en16155767"><u>https://doi.org/10.3390/en16155767</u></a>
- 16 P. A. Gbadega, Y. X. Sun, and K. T. Akindeji: 2024 32nd Southern African Universities Power Engineering Conf., Saupec (2024) 1. <a href="https://doi.org/10.1109/Saupec60914.2024.10445027">https://doi.org/10.1109/Saupec60914.2024.10445027</a>
- 17 X. L. Zhang, H. X. Wu, M. T. Zhu, M. W. Dong, and S. F. Dong: Energies 17 (2024) 1255. <a href="https://doi.org/10.3390/en17051255"><u>https://doi.org/10.3390/en17051255</u></a>
- 18 C. L. Wang and X. Li: Sci. Rep. 14 (2024) 16034. https://doi.org/10.1038/s41598-024-66492-1
- 19 R. D. Liu, S. Zhang, Y. C. Zhao, H. J. Ma, L. Chen, W. H. Hu, M. Tang, W. Zhan, and Q. J. Zhou: 2024 6th Asia Energy and Electrical Engineering Symp., AEEES 2024 (2024) 248. <a href="https://doi.org/10.1109/Aeees61147.2024.10544963">https://doi.org/10.1109/Aeees61147.2024.10544963</a>
- H. Wang, H. J. Xing, Y. F. Luo, and W. B. Zhang: Int. J. Electr. Power Energy Syst. 144 (2023) 108602. <a href="https://doi.org/10.1016/j.ijepes.2022.108602">https://doi.org/10.1016/j.ijepes.2022.108602</a>